

# Optical manifestation of the Stoner ferromagnetic transition in 2D electron systems

A. B. Van'kov,<sup>1,2</sup> B. D. Kaysin,<sup>1</sup> and I. V. Kukushkin<sup>1,2</sup>

<sup>1</sup>*Institute of Solid State Physics, RAS, Chernogolovka 142432, Russia*

<sup>2</sup>*National Research University Higher School of Economics, Moscow, 101000, Russia*

(Dated: April 29, 2022)

We perform a magneto-optical study of a two-dimensional electron systems (2DES) in the regime of the Stoner ferromagnetic instability for even quantum Hall filling factors on  $\text{Mg}_x\text{Zn}_{1-x}\text{O}/\text{ZnO}$  heterostructures. Under conditions of Landau-level crossing, caused by enhanced spin susceptibility in combination with the tilting of the magnetic field, the transition between two rivaling phases—paramagnetic and ferromagnetic—is traced in terms of optical spectra reconstruction. Synchronous sharp transformations are observed both in the photoluminescence structure and parameters of collective excitations upon transition from paramagnetic to ferromagnetic ordering. Based on these measurements, a phase diagram is constructed in terms of the 2D electron density and tilt angle of the magnetic field. Apart from stable paramagnetic and ferromagnetic phases, an instability region is found at intermediate parameters with the Stoner transition occurring at  $\nu \approx 2$ . The spin configuration in all cases is unambiguously determined by means of inelastic light scattering by spin-sensitive collective excitations. One indicator of the spin ordering is the intra-Landau-level spin exciton, which acquires a large spectral weight in the ferromagnetic phases. The other—is an abrupt energy shift of the intersubband charge density excitation due to change in the many-particle energy contribution upon spin rearrangement. From our analysis of photoluminescence and light scattering data, we estimate the ratio of surface areas occupied by the domains of the two phases in the vicinity of a transition point. In addition, the thermal smearing of a phase transition is characterized.

PACS numbers: 71.27.+a, 73.20.Mf, 73.43.-f, 78.67.-n

## I. INTRODUCTION

Two-dimensional electron systems (2DES) with strong interaction have attracted considerable research attention from the perspective of fundamental physics. The technological perfection of novel 2D materials extends their parameter space far beyond the framework of GaAs-based heterostructures. Interesting examples include 2D Fermi liquids in ZnO-based heterostructures, which exhibit an unusual combination of a large value of the interaction parameter  $r_s$  with ultrahigh electron mobility level<sup>1,2</sup>. New correlated states in magnetic fields may appear as a result of the interplay between key energy scales: cyclotron, Zeeman splitting, and inter-particle Coulomb energy. The material parameters of ZnO-based structures with 2DES facilitate close proportion between energy scales in magnetic fields: Zeeman splitting ( $g_{bulk}^* \sim 2$ ) and cyclotron energy ( $m_{bulk}^* \sim 0.28 m_0$ ). At moderate magnetic fields, the Coulomb energy has a substantially higher scale, thus resulting in high values of the Landau level (LL) mixing parameter and entangling the familiar single-particle energy spectrum. Nevertheless, the energy level sequence may be partially restored if renormalization of Fermi-liquid parameters is taken into account. In this context, in previous works, a substantial renormalization of the electron effective mass and spin susceptibility has been observed in ZnO at large values of the interaction parameter  $r_s$ .<sup>3-5</sup> As a result, opposing spin levels of adjacent LLs may approach closer to each other in terms of energy than those of the same LL. If they happen to intersect, spontaneous symmetry breaking between two rivaling spin configurations is possible.

At integer Landau level fillings, the corresponding phases are called quantum Hall ferromagnets (QHF) and can be treated within the confines of the Ising model. Experimentally, this Ising ferromagnetic (FM) transition is triggered either by tuning the electron's spin susceptibility, or if the spin splitting is not sufficiently large, by tilting the external magnetic field at definite *coincidence* angles.

The appropriate coincidence angles can be estimated from the following simplified single-particle relation:

$$\frac{E_z}{\hbar\omega_c} = \frac{g^*m^*}{2 \cos \Theta} = j, \quad (1)$$

where  $g^*m^*$  represents the effective spin susceptibility,  $\Theta$  the tilt angle of the magnetic field, and integer  $j$  the coincidence index. This formula has been regularly utilized in magnetotransport experiments for probing the spin susceptibility, but it lacks accuracy due to the influence of the many-particle interaction on the spin splitting and effective mass. Its applicability at small integer or fractional filling factors is violated due to the strong exchange effects, which lead to modification of the energy spectrum<sup>5,6</sup>. The physics of fractional quantum Hall states may be also modified by level crossing, though in this case levels of composite fermions play the role. In particular, certain unknown even-denominator fractional states have been detected in ZnO-based 2DES<sup>6</sup> at tilt angles different from single-particle values obtained from Eq.(1).

The physics of Ising QHF at small integer filling factors is essentially a many-body problem, since it is governed by the exchange interaction. As has been estab-

lished earlier in a series of magnetotransport studies of 2DESs in different heterostructures<sup>7–10</sup>, a Stoner ferromagnetic transition at integer filling factors involves the formation of domains. The transition point itself was identified by the appearance of sharp resistance spikes, although important physical parameters such as the energy spectrum of the different phases, areas occupied by them, and the stability of domains remained unknown.

In this context, here, we present the first optical study of a Stoner ferromagnetic transition in a set of ZnO-based heterostructures with 2DESs in the regime corresponding to the integer quantum Hall effect. Transformations of the  $\nu = 2$  ground state are carefully studied, and consonant events for filling factors of 3, 4 and 6 are also traced. The conditions for a Stoner transition are determined in view of abrupt transformations in the 2DES energy spectra. Qualitative reconstruction is detected both in the magneto-photoluminescence (magneto-PL) spectrum and parameters of the electronic collective excitations, as probed by inelastic light scattering (or the Raman) technique. The phase diagram of Ising QH ferromagnets at  $\nu = 2$  is acquired in terms of the critical tilt angle as a function of the electron density. Three essential regions are identified in the diagrams: stable paramagnetic (PM) region, FM region and an instability region, wherein the Stoner transition takes place at  $\nu \approx 2$ . At electron densities of  $n_s < 2 \times 10^{11} \text{ cm}^{-2}$ , FM order is observed to spontaneously develop even at normal orientation of the magnetic field. From an analysis of the PL and Raman spectra, the ratio of areas occupied by the domains of the two rivaling phases across the transition point is estimated. Furthermore, the domain sizes and their thermal stability are probed.

## II. EXPERIMENTAL TECHNIQUE

Measurements were performed on a series of  $\text{Mg}_x\text{Zn}_{1-x}\text{O}/\text{ZnO}$  heterostructures grown by liquid-ozone-assisted molecular beam epitaxy<sup>1</sup>. Each structure contained a high-quality 2D electron channel of varying density, as defined by the Mg-content in the barrier. Key parameters of the as-grown samples were characterized by magnetotransport analysis and are summarized in Table I.

Experiments were conducted at low temperatures in the range of 0.3 – 4.2 K using the  $\text{He}^3$  evaporation inset to the cryostat with a superconducting solenoid. Samples were mounted on a rotational stage in order to control their orientation with respect to the magnetic field direction. Tilt angles were tuned *in situ* with discrete steps with a finesse of  $\sim 0.5^\circ$ . The applied magnetic fields spanned the range of 0 to 15 T.

Optical access to the sample was established via two quartz fibers, one of which was used for photoexcitation, while the other was used for signal collection. This optical scheme benefits from a higher signal output and the absence of background parasitic scattering from the

TABLE I: Parameters of two-dimensional electron system (2DES) in the set of studied samples in order of increasing electron density. The electron density  $n_s$  was measured using the magneto-photoluminescence technique. Mobility  $\mu_t$  was qualified by magnetotransport measurements.

| Sample ID | $n_s$ ( $10^{11} \text{ cm}^{-2}$ ) | $\mu_t$ ( $10^3 \text{ cm}^2/\text{V}\cdot\text{s}$ ) |
|-----------|-------------------------------------|-------------------------------------------------------|
| 254       | 1.14                                | 710                                                   |
| 259       | 1.8                                 | 570                                                   |
| 244       | 2.3                                 | 400                                                   |
| 427       | 2.8                                 | 427                                                   |
| 426       | 3.5                                 | 410                                                   |
| 448       | 4.5                                 | 250                                                   |

fiber core. The angle configuration of the fibers determines the momentum transferred from light to the 2DES. Photoexcitation was produced by a tunable laser source operating in the vicinity of the direct interband optical transitions of ZnO. The laser source was designed as a frequency-doubled tunable continuous-wave Ti-sapphire laser with output monochromatic radiation in the wavelength range of 365 to 368 nm. A barium borate crystal set in the single-pass configuration was utilized as a non-linear element. The typical UV excitation power was 2–7  $\mu\text{W}$ , which was distributed over an excitation spot with a surface area  $\sim 1 \text{ mm}^2$ . Thus, the excitation power density was well below 1  $\text{mW}/\text{cm}^2$ , and which prevented the heating of 2D electrons. Optical spectra were detected with the use of a spectrometer in conjunction with a liquid-nitrogen-cooled CCD-camera. In the UV range, the system exhibited a linear dispersion of 5  $\text{\AA}/\text{mm}$  and spectral resolution of 0.2  $\text{\AA}$ .

The dynamics of each sample was extensively studied with respect to the magnetic-field orientation in order to study the recombination spectrum transformation in the vicinity of integer filling factors. In addition, PL was utilized for electron density characterization, as described previously<sup>12</sup>, and for determining the resonant conditions of inelastic light scattering.

Inelastic light scattering signal was studied predominantly at magnetic fields corresponding to LL filling factors of  $\nu = 2$ ,  $\nu = 1$ , and values in between. The multitude of spectral lines was dominated by a PL signal residing at stationary wavelength positions, and it was not affected by laser tuning. Raman lines, although weak, could be distinguished by their constant energy shift from the sweeping laser position. An important observation here is that the intensities of the Raman features from 2D electrons behave resonantly while crossing definite PL bands. This trick has been thoroughly described in the previous paper, devoted to collective excitations in ZnO-based 2DESs at zero magnetic field<sup>13</sup>. Here, at high magnetic fields, the Raman line search procedure was essentially the same as in the previous study, and only the resonant contours were slightly shifted by the applied magnetic field.

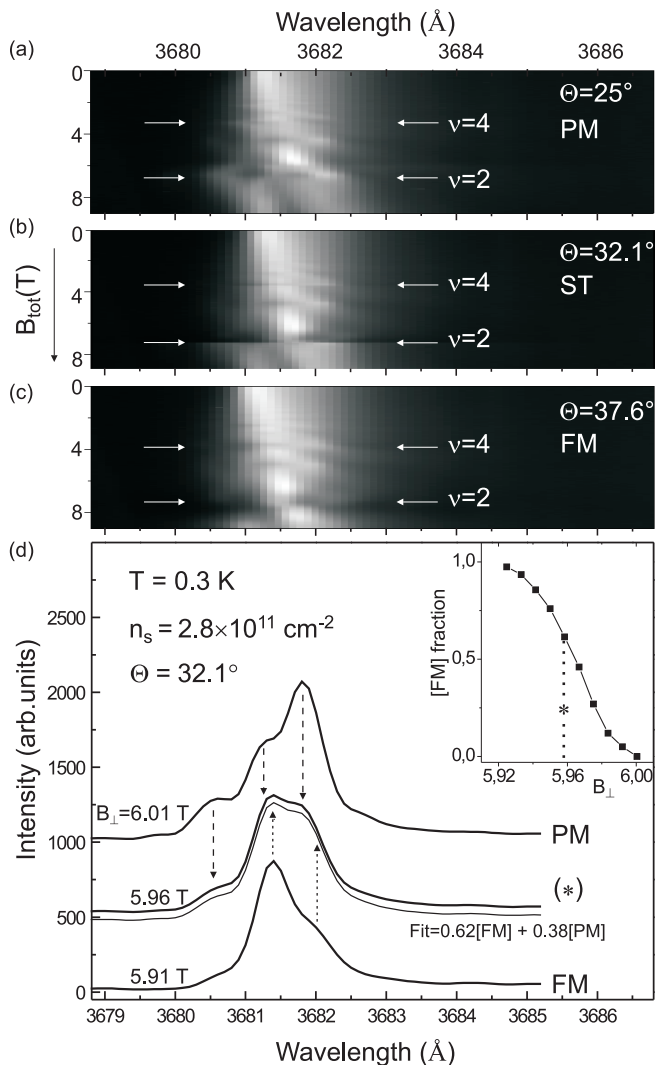


FIG. 1: (a), (b), and (c) – Image plots of the photoluminescence (PL) magnetic-field dynamics of the 2DES in MgZnO/ZnO heterostructure with  $n_s = 2.8 \times 10^{11} \text{ cm}^{-2}$  measured at three sample orientations  $\Theta$ , corresponding to qualitatively different behaviors at even filling factors: (a) paramagnetic, (b) Stoner transition, and (c) ferromagnetic ordering. Positions with distinctive PL behavior at  $\nu = 2$  and 4 are indicated by double horizontal arrows. In panel (b), cutoff positions are discernible by image discontinuity. (d) Modification of PL spectra around  $\nu = 2$  at ferromagnetic and paramagnetic phases and their superposition at a Stoner transition point (cutoff field). In all cases, the temperature of the sample was close to 0.3 K. The inset illustrates a fraction of the ferromagnetic phase as a function of the magnetic field around the transition point, as extracted from the superposition fit. The asterisk marks the position of the cutoff field.

### III. OPTICAL RESPONSE OF QUANTUM HALL FERROMAGNETS

The first indication of the rearrangement in LLs is manifested in the modification of the magneto-

photoluminescence dynamics. Figures 1 a-c present the PL evolution of the 2DES in Sample 427 (density  $n_s = 2.8 \times 10^{11} \text{ cm}^{-2}$ ) as image plots with the magnetic field increasing along the downward y-direction. The dynamics shown in panel (a) ( $\Theta = 25^\circ$ ) and those at smaller angles are all nearly equivalent if corrected to the normal component of the magnetic field. They represent smooth  $1/B_\perp$ -periodic oscillations of the PL-intensity at spectral positions close to the Fermi level as the 2DES transitions through conventional quantum Hall states<sup>12</sup>.

On further tilting of the field, we suddenly observe a qualitatively different behavior: the spectral dynamics undergoes abrupt transformations at magnetic field values close to filling factors  $\nu = 2, 4, 6, \dots$ . On the high-field side of this cutoff ( $B^*$ ), the PL evolution coincides with the previous case of Fig. 1a, but at smaller fields, the spectrum undergoes a sudden "reorganization": two narrow peaks emerge instead of three, and their oscillator strengths become inverted (See top and bottom spectra in Fig. 1d). The high-energy spectral line centered at  $\sim 3680.5 \text{ \AA}$  for  $\nu = 2$  and also developed at other even filling factors completely disappears (see Fig. 1a). This "reconstruction" of the PL spectrum is indicative of the abrupt magnetic-field-driven change in the ground state. The range of these *critical* tilt angles supporting such transformations is a few degrees, exceeding which the dynamics becomes "smooth" again with the modified recombination spectrum close to even filling factors (See panel (c) on Fig. 1). Importantly, this new appearance of spectra at even filling factors (the lowest spectrum on Fig. 1d) is identical to those at  $B < B^*$  near the cutoff (Fig. 1b) and thus represents the PL signature of the new phase of the  $\nu = 2$  state. At tilt angles supporting abrupt PL transformations, the 2DES undergoes a phase transition. As discussed below and in accordance with previous magnetotransport results<sup>4,6</sup>, the two phases around  $\nu = 2$  correspond to PM ordering with opposite LL spin states equally occupied and FM ordering with inverted spin orientation of the highest occupied spin level. For the sake of brevity, the PL spectra of different phases in Fig. 1 are denoted as PM and FM. An interesting interplay between the two phases can be observed across the narrow B-field transition region. Here, the resulting spectrum is composed of the superposition of the PM and FM spectra (Fig. 1d). The proportion between the phases is gradually switched from the full PM to the full FM state over a span of  $\Delta B < 0.1 \text{ T}$ . An example of the best linear superposition fitting the mixed PL spectrum is overlaid on the middle spectrum in Fig. 1d, and the relative weights are plotted in the inset therein. This system state witnesses the co-existence of domains in a narrow transition region of magnetic fields and facilitates direct estimation of the phase percentage.

Similar experiments were performed on all other samples listed in Table I with electron densities ranging from  $1.14 \times 10^{11}$  to  $4.5 \times 10^{11} \text{ cm}^{-2}$ . The data are consolidated on a plot with critical angles as a function of the electron density (Fig. 2). Qualitatively similar behavior

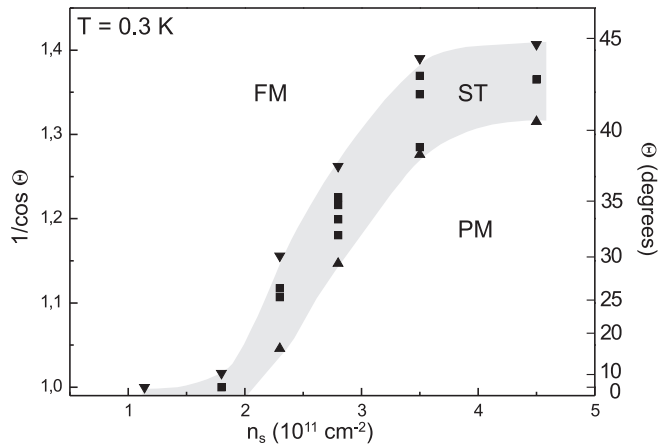


FIG. 2: Phase diagram of Ising quantum Hall ferromagnets at  $\nu \approx 2$ , obtained as a plot of the magnetic field tilt angle versus electron density. Ranges corresponding to ferromagnetic and paramagnetic phases and the Stoner instability region are specified. Experimental symbols corresponding to each of the samples mark the boundary tilt angles between different regions (upward and downward triangles) and a few angles in between corresponding to the Stoner transition. The shaded region, encompassing the instability region, serves as a visual guide. For the lowest density sample with  $n_s = 1.14 \times 10^{11} \text{ cm}^{-2}$ , the paramagnetic phase at  $\nu = 2$  is absent, and the Stoner ferromagnet is observed at all tilt angles.

was observed for all the 2DESs with densities exceeding  $2 \times 10^{11} \text{ cm}^{-2}$ , corresponding to three regions with different magneto-PL dynamics around even filling factors. However, the angles strongly depend on the electron density due to the Fermi-liquid renormalization of the spin susceptibility. At  $n = 1.8 \times 10^{11} \text{ cm}^{-2}$ , the Stoner transition around  $\nu = 2$  occurs even for the normal orientation of the magnetic field. The instability region spans  $\Theta \sim 10^\circ$ . At even lower densities, a stable Stoner ferromagnet is formed even at normal magnetic fields. Although the phase diagram corresponds to the quantum Hall state  $\nu = 2$ , these conditions perfectly correlate with transformations at other even filling factors. In addition, the level crossing with index  $j = 2$  (from Eq.(1)) was observed for  $\nu = 3$  for the sample with density  $2.8 \times 10^{11} \text{ cm}^{-2}$ . The tilt angles for this second coincidence lie in the very narrow range of  $\Theta_2 = 63.5 \pm 0.5^\circ$ , and this result is consistent with the results of magneto-transport experiments for higher coincidence indices and filling factors. This behavior may be attributed to less pronounced exchange effects in level crossing.

An extended view of these phenomena was obtained by means of inelastic light scattering experiments. Here, we expected the probing of collective excitations to reveal the spin properties of the ground state. As reported in the previous study<sup>13</sup>, inelastic light scattering signal corresponding to neutral electronic excitations of 2DES can be found in vicinity of its PL recombination lines. The point of interest here is the estimation of appropriate

resonance conditions for each Raman spectral line and its further identification. Data obtained in<sup>13</sup> for zero magnetic field can be utilized to identify the set of inter-subband excitations at any given magnetic field simply by tracing the resonances while continuously increasing magnetic field. In the context of the Stoner transition, most actual are the excitations, sensitive to the spin-degree of freedom. The direct sensor is an intra-LL spin exciton (SE) – collective mode, indicative of a spin arrangement. Irrespective of the inter-particle correlations, the energy of the SE is close to pure Zeeman splitting in the long-wavelength case (Larmor’s theorem<sup>14</sup>). This property makes the SE trivial for identification. In our structures, this excitation appears in the Raman spectra over the comparatively wide range of laser wavelengths of  $\sim 9\text{\AA}$ , overlapping with the resonant conditions for an intra-LL magnetoplasmon. Over a wide span of the magnetic field, the SE energy increases linearly with an effective Lande factor  $g^* = 2.00 \pm 0.015$  (plot in Fig.3b). A feature of interest with regard to this excitation is its most elementary structure with just one quantum number (the total 2DES spin) changed by unity. This hinders the decomposition of the SE into other elementary excitations even when the system deviates from incompressible states. For this reason, the SE is a ”long-lived” excitation, and its spectral width in the actual Raman spectra is determined solely by the equipment resolution of  $\sim 0.2 \text{ meV}$ , rather than its thermal decay and inhomogeneous broadening. The typical SE Raman spectrum is shown in Fig.3a.

The most indicative property of the SE is the change in its spectral intensity with change in the spin ordering in the system. According to the trivial spin-flip representation of SE, its weight is obviously proportional to the number of occupied states in the initial spin level and the number of vacancies in the final level. Therefore, the SE should gain the maximum weight in systems with FM ordering and conversely zero weight in the PM phases corresponding to normal states with even filling factors. A quantitative analysis of the SE spectral intensity behavior at arbitrary filling factors is hardly possible, since it would require knowledge of the microscopic structure of the ground state and consideration of the orbital wave functions of participating electrons. Nevertheless, the experimental dynamics of the SE line intensity can serve as an indicator of the general asymmetry in the spin-up and spin-down occupations and is particularly meaningful in the vicinity of integer QH states.

Fig.4a depicts the magnetic field dynamics of the SE intensity in the sample with density  $n_s = 2.8 \times 10^{11} \text{ cm}^{-2}$  at the three angular orientations matching those of Fig.1. The horizontal axis represents the normal component of the magnetic field such that the positions of integer filling factors for all angles match each other. We note (in Fig.4a, angle  $25^\circ$ ) that in the ferromagnetic QH state at  $\nu = 1$ , the intensity reaches a local maximum as per the abovementioned considerations. Close to  $\nu = 2$ , the SE spectral weight reduces and abruptly drops to zero over

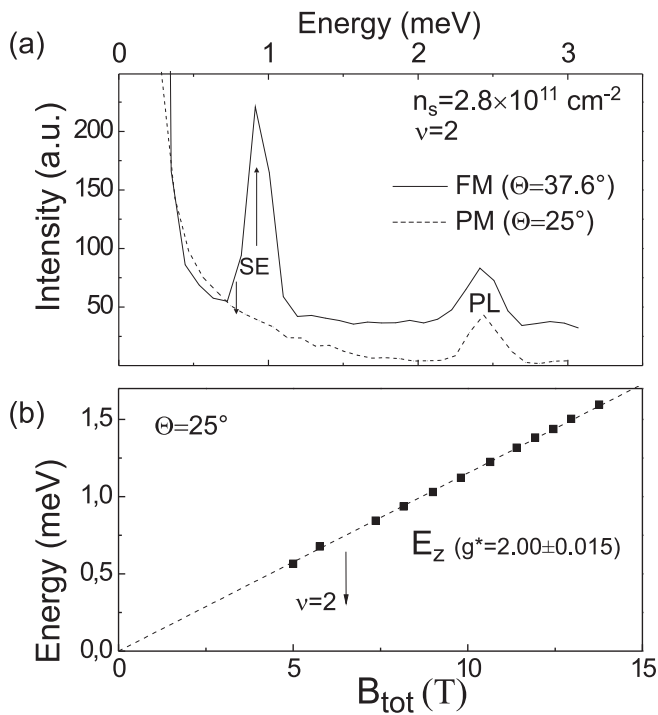


FIG. 3: (a) Raman spectra of spin exciton at  $\nu = 2$  and  $T = 0.3\text{K}$  at two different tilt angles, corresponding to the ferromagnetic and paramagnetic phases (the SE is absent in the PM phase). Arrows indicate the spectral positions of the SE Raman line calculated for  $g^* = 2$ . Apart from Raman signal, a single photoluminescence line is present in the spectrum, which can serve as a reference intensity level. (b) Energy of SE measured as a function of the total magnetic field for sample orientation of  $\Theta = 25^\circ$ .

a certain range on both sides of  $\nu = 2$ . Naturally, in this PM phase with symmetric occupation of the spin-up and spin-down states, the spin exciton is absent. Spontaneous symmetry breaking occurs around  $\nu = 2$  at a higher angle, corresponding to the Stoner instability region ( $\Theta = 32.1^\circ$  in Fig.4a). Here, the intensity of the SE spectral line suddenly increases and reaches a sharp maximum, thereby indicating the presence of parallel spin alignment in the system. Interestingly, on the right-hand-side region of  $\nu = 2$ , the SE intensity, although it drops dramatically, does not become zero, and therefore, the PM order is not entirely "resumed" here. The position of this cutoff in the SE behavior at angle  $\Theta = 32.1^\circ$  coincides with the discontinuity observed in the magneto-PL dynamics and evidently separates the two phases. The highest tilt angle for this sample ( $37.6^\circ$ ) corresponds to smooth dynamics both in the PL spectra and Raman spectra of the SE line. A pronounced local maximum in the SE intensity is observed right at  $\nu = 2$ , evidencing FM ordering of the 2DES. Apart from this feature, we can also notice a qualitatively similar behavior of the SE on the higher-magnetic-field side of  $\nu = 2$  at all angles. Taking this observation into account, we conclude that system first undergoes a spontaneous symmetry breaking

close to  $\nu = 2$ , which manifests as a discontinuity in the energy spectrum at tilt angles in the instability range. The spin ordering at fields slightly exceeding the transition point deviates from paramagnetic and is not fully compensated, probably due to the nucleation of the FM phase. For angles lying outside this range, the Stoner transition does not occur; instead, the whole neighborhood of  $\nu = 2$  corresponds to the FM phase.

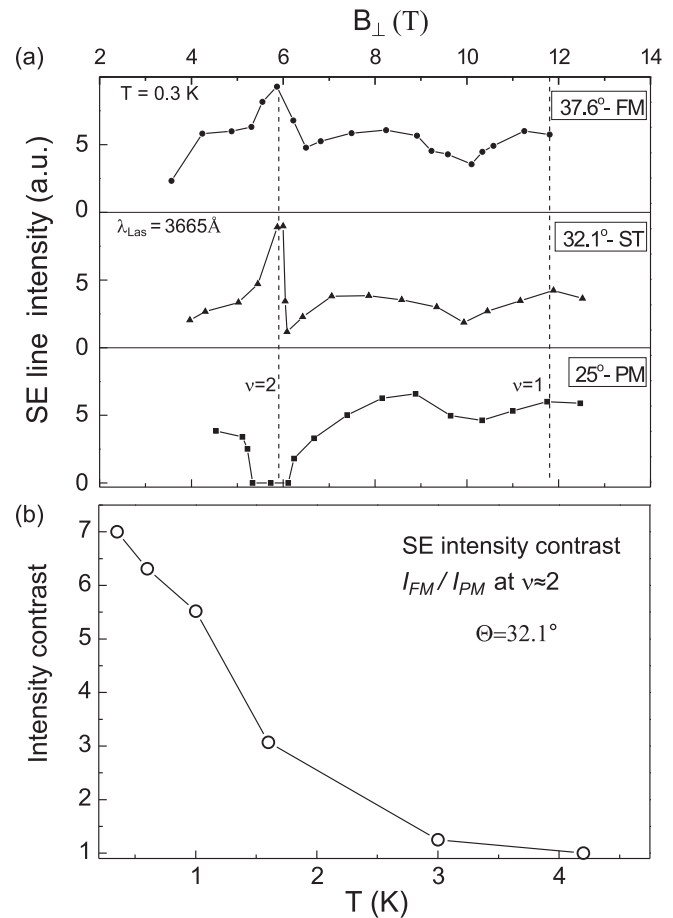


FIG. 4: Behavior of intra-Landau-level spin exciton spectral intensity as a function of the spin transformations at  $\nu \approx 2$  in the sample with  $n_s = 2.8 \times 10^{11}\text{cm}^{-2}$ . (a) The magnetic field dependence of the SE spectral intensity as recorded for three different tilt angles. In the paramagnetic (PM) phase ( $\Theta = 25^\circ$ ), the SE is absent near  $\nu = 2$ , in the ferromagnetic (FM) phase ( $\Theta = 37.6^\circ$ ), its intensity exhibits a local maximum, and at the Stoner transition ( $\Theta = 32.1^\circ$ ), the SE behavior sharply switches between the PM and FM cases. In all cases, the SE spectral intensity reaches maximum again in the QHF state of  $\nu = 1$ . (b) The temperature dependence of the SE line intensity ratio on either side of the cutoff field, recorded at angle  $\Theta = 32.1^\circ$ .

The dramatic change in SE intensity across the Stoner transition point can be considered as an indicator of a phase contrast between PM and FM orderings. The thermal stability of these phases was next probed in terms of the "smearing" of the SE intensity collapse. At a fixed tilt

angle and varying temperatures, the intensity contrast  $I_{FM}/I_{PM}$  was calculated as the ratio of the SE intensities corresponding to the local maximum (FM phase) and the local minimum (PM phase) near  $\nu = 2$ . The dynamics of this value was measured in the temperature range 0.3...4.2K (see Fig.4b). From the figure, we note that the intensity contrast drops with decrement corresponding to  $\sim 2$  K. Effectively, the temperature  $T=1.6$  K is the last temperature value at which the Stoner-like discontinuity is observed. This result affords an estimate of the Curie temperature for these QHF states, which was also characterized in magnetotransport experiments as the limiting temperature at which the domains of the two phases exist in the system<sup>8</sup>.

An additional tool sensitive to local spin configuration is represented by the energy of the long-wavelength collective excitations. Recently, the intersubband plasmon (or charge density excitation - CDE) has been shown to reflect the spin-polarization degree owing to changes in the exchange energy contribution<sup>15</sup>. Being not particularly susceptible to LL occupation, this intersubband mode nevertheless exhibits a qualitatively different structure between FM and PM spin orderings. A considerable shift in the CDE energy ( $\sim 1$  to 2 meV) has been detected in several ZnO-based structures while continuously tuning the system from an unpolarized  $\nu = 2$  state to the FM state  $\nu = 1$ . In view of our study, the energy shifts of the intersubband CDE at  $\nu = 2$  behave in accordance with the spin transformations. First of all, the CDE energy in the  $\nu = 2$  PM phase at small tilt angles is equal to that at  $B=0$  T or high LL filling factors. An identical CDE spectrum is observed on the high-field-side of the cutoff point at tilt angles in the instability range (see the topmost spectrum in Fig.5c and lower-energy data symbols in Figs.5a and 5b). This is clear evidence that the spin-unpolarized states possess intersubband CDE with equal energies. The abrupt shift in the CDE energy occurs while tuning the magnetic field across the cutoff point (the lowest spectrum in Fig.5c). This spectrum is identical with that in the neighborhood of  $\nu = 2$  at tilt angles lying in the FM region, and most interestingly, it is similar to that of the FM state at  $\nu = 1$ . This situation is illustrated in Figs.5a and 5b, corresponding to two samples with different densities. The CDE energies on both sides of the Stoner transition are aligned to those at the FM  $\nu = 1$  state (where it is accessible by the solenoid) and  $B=0$  T. Furthermore, the two CDE lines are observed simultaneously in the narrow range of fields across the Stoner transition (the middle spectrum in Fig.5c). This means that a surface-integrated Raman signal contains the linear superposition of separate spectra from the two phases. This information is valuable since the presence of unperturbed energies of the collective excitations, emanating from the domains of different phases, is possible provided their sizes exceed at least few magnetic lengths. In general, this conclusion agrees with theoretical expectations based on the Ising model<sup>11</sup>.

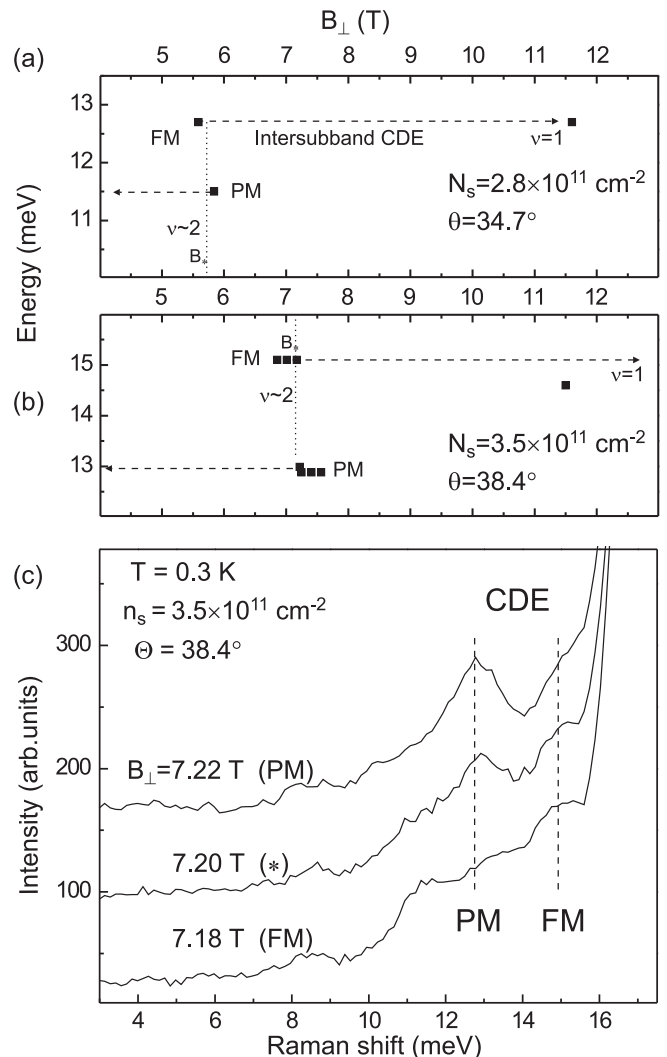


FIG. 5: (a) and (b) Energies of intersubband charge density excitation (CDE) measured for two different samples at tilt angles supporting Stoner transition. The sharp energy shift at  $\nu \approx 2$  is due to spin rearrangement at the ferromagnetic-paramagnetic (FM-PM) phase transition. Horizontal dashed lines are intended to align CDE energies on either sides of  $\nu = 2$  to those of spin-polarized ( $\nu = 1$ ) and spin-unpolarized (zero magnetic field) states. (c) Raman spectra of intersubband CDE in the sample with  $n_s = 3.5 \times 10^{11} \text{ cm}^{-2}$  at three closely lying magnetic field values around the Stoner transition point. The CDE lines at two energy positions are interplayed in intensity according to the phase proportion. Their positions are marked with vertical dashed lines.

#### IV. DISCUSSION

The control of the spin configuration at integer filling factors by means of magnetic field tilting was shown to differ from the single-particle considerations. A wide range of tilt angles is suitable for affording a level coincidence at even filling factors. This implies a substantial exchange contribution in the coincidence condition. For

this reason, the phase diagram of QHFs in terms of critical tilt angles at even filling factors contains three essential regions: stable PM phase with anti-parallel spin orientation, stable FM phase with a pronounced maximum of spin polarization at even filling factors, and an instability region supporting a phase transition near even filling factors. Fermi-liquid effects, dependent on electron density, cause substantial shift of the critical tilt angles. At densities lower than  $\sim 2 \times 10^{11} \text{ cm}^{-2}$ , the stable PM phase at  $\nu = 2$  is no longer accessible, and instead, a Stoner transition occurs at small angles. At even lower densities of  $\sim 10^{11} \text{ cm}^{-2}$ , the FM phases are stable independently of the tilt for at least several even filling factors  $\nu = 2, 4, \dots$

These sharp transformations of the 2DES phases are particularly amazing, bearing in mind the substantial macroscopic nonuniformity in the electron density, which is estimated to be  $\delta n_s \sim 5\text{-}10\%$ , depending on the sample. The Stoner transition appears to be governed by a certain coherent process, aligning a chemical potential level throughout the entire 2DES. Therefore, from the plot in the inset in Fig.1d, we note that the entire transition fits in less than  $\delta B \sim 0.1 \text{ T}$ , within  $\sim 1.5\%$  of the whole field. The range of fields, extracted from the SE intensity drop, correlates with that of the PL transformation. The proportion of the two phases is most effectively extracted from the PL-spectra interplay, since the PM and FM phases have specific signatures and in addition provide a strong signal. This approach can also aid in characterizing the subtle hysteretic behavior of the Stoner transition at  $T = 0.3 \text{ K}$ . So, the sweep-direction difference in the cutoff positions was of the order  $0.01 \text{ T}$  for sample 427 with density in the middle of the studied range. This is likely due to the easy-moving domain walls in low-disorder systems.

The non-vanishing SE Raman line on the higher-field side of the transition region corresponds to residual asymmetry in spin occupation despite signs of a dominant PM phase. This is most probably due to the nucleation of the FM phase, which is however too sparse to be discernible in the PL-spectra distortion or modification of the CDE mode. This fact contradicts the existing hypothesis concerning pure spin states on either side of the Stoner transition point<sup>6,9</sup>. The SE is particularly sensitive to perturbations of spin-unpolarized states, since its intensity is better traced on a zero background. The symmetrical situation with nucleation of the minority phase is possible at fields in the FM region. However the SE intensity can hardly serve for detection of this, since intensity deviations should have been counted from an unknown maximum intensity level.

The SE line at other even filling factors ( $\nu = 4, 6, \dots$ ) flashes in phase with ferromagnetic order, although its visibility is poorer than that of the FM state  $\nu = 2$  due to the stronger laser-line background. A qualitatively similar response was obtained for the phase transition between two spin configurations at  $\nu = 3$ . In this case, for coincidence angle  $\Theta_2 = 63.5^\circ$ , the SE intensity drops by

a factor of  $\sim 2.4$  across the cutoff point. This value reasonably agrees with naive single-particle picture of spin-state occupation at this filling factor which corresponds to  $I_{max}/I_{min} = 3$ .

The thermal degradation of the SE contrast at a Stoner transition qualitatively shows that domains with rivaling phases undergo melting at temperatures of  $\sim 2 \text{ K}$ , which value is significantly lower than Zeeman and exchange energies, but it appears to be comparable with the Curie temperature estimated for an easy-axis QHF in terms of domain-wall excitations<sup>11</sup>  $T_C \sim 0.009 e^2/\epsilon\ell_B$ . This calculation as applied to sample 427 at  $\nu = 2$ ,  $B_\perp = 5.9 \text{ T}$ , and  $\epsilon = 8.5$  yields  $T_C \sim 1.6 \text{ K}$ . It is also worth noting that at temperatures above  $4 \text{ K}$ , the behavior of the SE intensity as a function of the magnetic field is absolutely flat, with no peculiarities at integer QH states.

Concerning the domain size, the SE line is of no utility since it reflects a general asymmetry in spin occupation. More indicative of the domain size are the energies of the collective modes. In our study, the observed inter-subband CDE energy shift indicates that at a transition point, the macroscopic QH domains of different phases coexist and that their sizes exceed few magnetic lengths, since a collective mode has unperturbed energy and spectral width. According to theoretical expectations<sup>11</sup>, at a transition point (resistance spike maximum in magneto-transport), the typical domain sizes are about dozens of magnetic lengths, but on deviation from the transition point by an effective magnetic field of  $\delta B \sim 0.02 \text{ T}$ , the minority phase domains shrink to a size of  $\sim 3 \ell_B$ . This result is consistent with our conclusion, since at small deviations from the central field of the Stoner transition, the minority phase CDE line vanishes (Fig.4c).

## V. CONCLUSION

In conclusion, we performed a magneto-optical study of the Stoner transition between quantum Hall ferromagnetic states in 2D electron systems based in MgZnO/ZnO heterostructures. Abrupt transformations were detected both in the photoluminescence spectra and in 2D collective excitations, probed by resonant inelastic light scattering. The transition was facilitated by the tilting of the magnetic field, thus bringing spin-Landau levels to coincidence. Depending on the 2D electron density, the spin configuration varied at different critical angles. This phenomenon was exploited to draw the phase diagram for quantum Hall ferromagnets at  $\nu \sim 2$  in terms of the tilt angle vs 2D electron density. Three qualitatively different regions were identified: a stable paramagnetic phase around even filling factors, a stable ferromagnetic phase, and a Stoner instability region in between. At low electron densities of  $\sim 1 - 2 \times 10^{11} \text{ cm}^{-2}$ , Fermi-liquid effects lead to a Stoner transition even at normal magnetic field orientation. The spin configuration at each state was characterized via the spectral weight of the intra-Landau-level spin exciton. The spin exciton inten-

sity displays a maximum-like behavior in the vicinity of the ferromagnetic states. At a Stoner transition point near  $\nu = 2$ , it switches from a sharp maximum (in the ferromagnetic phase) to a deep minimum (paramagnetic phase). However, it does not vanish completely, thereby indicating the presence of some ferromagnetic nucleation in the paramagnetic state. From thermal smearing of the spin exciton dynamics, the Curie temperature of quantum Hall ferromagnets was estimated to be  $\sim 2$  K. Optical signals from the domains were observed to superimpose, which facilitated the direct calculation of the phase proportions across the transition point. It was also shown

that intersubband collective excitations from the two different phases coexist at the transition point and are unperturbed, thus indicating that the domain sizes exceed few magnetic lengths.

### Acknowledgments

We acknowledge financial support from the Russian Scientific Foundation (Grant No.14-12-00693).

- 
- <sup>1</sup> J. Falson, Y. Kozuka, J. H. Smet, T. Arima, A. Tsukazaki and M. Kawasaki, Applied Physics Letters **107**, 082102 (2015).
- <sup>2</sup> Y. Kozuka, A. Tsukazaki, and M. Kawasaki, Applied Physics Reviews, **1**, 011303 (2014).
- <sup>3</sup> A. Tsukazaki, A. Ohtomo, M. Kawasaki, et al., Phys.Rev.B **78**, 233308 (2008).
- <sup>4</sup> Y. Kozuka, A. Tsukazaki, D. Maryenko, J. Falson, C. Bell, et al., Phys.Rev.B **85**, 075302 (2012).
- <sup>5</sup> D. Maryenko, J. Falson, Y. Kozuka, A. Tsukazaki, and M. Kawasaki, Phys.Rev.B **90**, 245303 (2014).
- <sup>6</sup> J. Falson, D. Maryenko, B. Friess, D. Zhang, Y. Kozuka, A. Tsukazaki, J. H. Smet and M. Kawasaki, Nature Physics **11**, 347 (2015).
- <sup>7</sup> E. P. De Poortere, E. Tutuc, S. J. Papadakis, M. Shayegan, Science **290**, 1546 (2000).
- <sup>8</sup> E. P. De Poortere, E. Tutuc, and M. Shayegan, Phys.Rev.Lett. **91**, 216802 (2003).
- <sup>9</sup> J. Jaroszynski, T. Andrearczyk, G. Karczewski, et al., Phys.Rev.Lett. **89**, 266802 (2002).
- <sup>10</sup> J. C. Chokomakoua, N. Goel, S. J. Chung et al., Phys.Rev. B, **69**, 235315 (2004).
- <sup>11</sup> T. Jungwirth and A. H. MacDonald, Phys.Rev.Lett. **87**, 216801 (2001).
- <sup>12</sup> V. V. Solovyev, A. B. Van'kov, I. V. Kukushkin, et al., Appl.Phys.Lett. **106**, 082102 (2015).
- <sup>13</sup> A. B. Vankov, B. D. Kaysin, V. E. Kirpichev, V. V. Solovyev, and I. V. Kukushkin, Phys.Rev. B **94**, 155204 (2016).
- <sup>14</sup> M. Dobers, K. von Klitzing, and G. Weimann, Phys. Rev. B **38**, 5453 (1988).
- <sup>15</sup> L.V. Kulik, A.B. Van'kov, B.D.Kaysin, and I.V. Kukushkin, JETP Letters, **105**, i.6, p. 358 (2017).